[SNS Moderators]
Chapter 2.3 in *Elements*)

Characterization of SNS moderators

Partly to facilitate comparisons between neutronic calculations and measurements of source performance and partly to facilitate neutron beam instrument design and calibration and data analysis, scientists appeal to model functions, described previously, with parameters fitted to measured or calculated data. We use results from the Spallation Neutron Source (SNS) at Oak Ridge National Laboratory as examples.

The moderators

The High Power Target Station (HPTS) of SNS has four moderators, two of which are viewed from both sides. The nominal 1-GeV proton beam power of HPTS is 2 MW, although the goal before completion of the full-power upgrade is 1.4 MW. The frequency of proton pulses is 60 Hz. The neutron-producing target is flowing liquid mercury, surrounded by a beryllium reflector. As this is written, SNS is operating at 1 MW. We cite performance figures for the current target and moderator configuration projected for 2-MW operation, that is, 34 kJ/pulse at 60 Hz.

Iverson et al. (2002) briefly describes the moderators and presents an array of figures based on Monte Carlo simulations. Here we focus on the moderators' time-average spectral intensities, pulse FWHMs, and mean emission times and introduce mathematical functions that fit the numerical simulations. The moderators provide six viewed surfaces to three beam lines each. Simulations result from calculations using the MCNPX code. Table 1 summarizes the description of the moderators. The reference provides further details of the moderators.

Table 1. Summary description of the SNS moderators
Numbering is counterclockwise from above, starting from the proton beam. Moderators are 100 mm wide and 120 mm tall.

Beamline Number	Case	Location[a]	Moderating material	Temper-ature	Decoupling material	Poison material	Poison depth	Overall thickness
2	#1	TU	H_2	20 K[b]	Cd	Gd	29.6 mm	60 mm[c]
11	#1	TU	H_2	20 K[b]	Cd	Gd	29.6 mm	60 mm[c]
5	#2	TD	H_2	20 K[b]	None	None	—	60 mm[c]
14	#2	BD	H_2	20 K[b]	None	None	—	60 mm[c]
8	#3	BU	H_2O	300 K	Cd	Gd	14.75 mm	40.5 mm
17	#4	BU	H_2O	300 K	Cd	Gd	24.75 mm	40.5 mm

[a] T: Top, above target; B: Bottom, below target; U: Upstream in proton beam direction; D: Downstream.
[b] Assumed 100% para-H_2.
[c] Maximum thickness. Curved viewed surface, average thickness 55 mm.

Of the six viewed moderator surfaces, two pairs are identical: beam line 2 and 11 from the TU moderator, and beam line 5 from the TD moderator and 14 from the BD moderator. We give results for the four distinctly different viewed moderator surfaces, with cases numbered as in T

Spectral intensities

Figure 1 shows the spectral intensities, that is, the time-integrated neutron total angular current per unit lethargy (the product of the energy E and the angular current per unit energy $I(E)$ per pulse), for the four distinctly different viewed moderator surfaces.

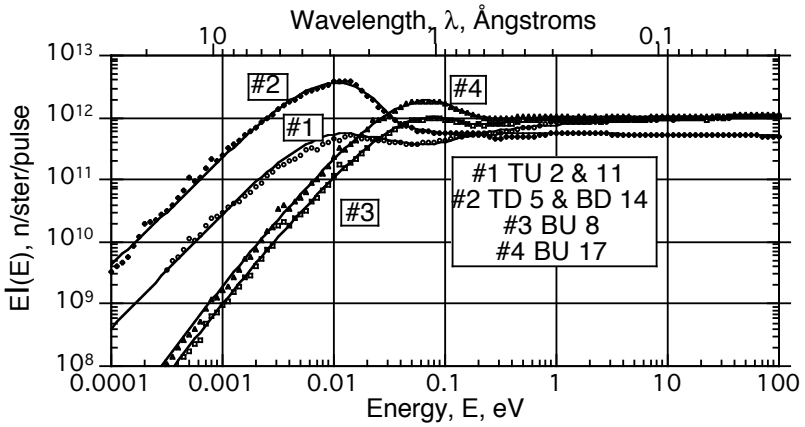

Figure 1. Calculated data and fitted functions of the spectral intensities of SNS moderators. (Data courtesy of E. B. Iverson.)

Modified Westcott functions fit the calculated data,

$$I(E) = I_{epi}\exp(-c/\sqrt{E})\left(R\frac{E}{(kT)^2}\exp(\frac{E}{kT}) + \Delta(E)\rho(E)\frac{1}{E}\left(\frac{E}{E_{\mathrm{Re}f}}\right)^{\alpha}\right). \quad (1)$$

We adopt this form, as Iverson et al. have used, rather than the simpler form proposed elsewhere because it can fit spectra of liquid hydrogen moderators. Here, $I(E)$ is spectral intensity, $I_{epi} = EI(E)\Big|_{E_{Ref}=1\ eV}$, $R = \frac{I_{Th}}{I_{epi}}$, I_{Th} is the integrated Maxwellian component, the first term in (1), $E_{Th} = k_B T$, T is the effective spectral temperature, and k_B is Boltzmann's constant. The factor $\exp\left(-\frac{c}{E}\right)$ is entirely empirical in origin, although it has the form for "1/v" attenuation. The generalized Westcott joining function is

$$\Delta(E) = \frac{1}{1+\left(\frac{E_{co}}{E}\right)^{s}} \quad (2)$$

in which E_{co} is the *cutoff energy* and s is the *cutoff exponent*. Brun's modification factor in (1), $\rho(E)$ (Brun 1998), enables fitting of spectra from liquid hydrogen moderators,

$$\rho(E) = 1 + \delta_p \exp(-x)\left(1 + x + \frac{x^2}{2}\right), \quad (3)$$

and

$$x(E) = \begin{cases} \gamma(E - 2B) \text{ for } E > 2B \text{ and} \\ \quad 0 \text{ for } E < 2B, \end{cases} \tag{4}$$

in which B is the free-H_2 rotational constant (B = 7.36 meV).

Table 2 displays the parameters of the functions fitted to the calculated spectra.

Table 2. Parameters of the calculated spectral functions
(Throughout, E_{Ref} = 1 eV.)

Beam lines	I_{epi} ,10^{11}, n/ ster/eV/pulse	$E_{th} = k_B T$ meV	R	c, $\sqrt{\text{eV}}$	E_{co}, meV	s	α	δ_p	γ, eV^{-1}
2 & 11	8.0	5.0	0.775	0.005	72	1.23	0.066	1.71	101
5 & 14	5.6	5.1	11.35	0.000	23	1.16	-0.018	0.73	51.5
8	9.3	32.	1.90	0.016	135	2.82	0.025	0.000	—
17	10.3	33.	3.60	0.017	155	4.89	0.012	0.000	—

The fitting functions are physics-inspired but not derivable from the theory of time-dependent neutron thermalization. Nevertheless, the fitted functions are reasonably accurate representations of the data, good to approximately ± 10%.

Pulse widths

The pulse FWHMs are the conventional measures of the pulse shape for assessment of resolution, because they relate in a simple way to plotted data. Standard deviations of the pulse emission time distributions are mathematically more useful because standard deviations of convoluted distributions, such as describe instrument performance, add in quadrature.

We have developed a new functional form that accurately fits the calculated pulse widths (and the emission time delays discussed next) as functions of the wavelength, similar to Padé approximants[‡] (ratios of polynomials) but generalized in that ours admit noninteger powers of the variable. There is but little physics motivating this form, except to incorporate the general trend toward proportionality to wavelength at short wavelengths and to level off to a power law dependence at long wavelength. The general form for the present purposes is

$$f(\lambda) = a\lambda^b \frac{1 + c\lambda + d\lambda^2 + \left(\frac{\lambda}{e}\right)^q}{1 + c'\lambda + d'\lambda^2 + \left(\frac{\lambda}{e'}\right)^{q'}} \ , \tag{5}$$

in which a, b, c, d, e, c', d', e', q and q' are fitting parameters and λ is the wavelength. Parameters e and e' enter to describe points of inflection in the fitted functions. We used a powerful nonlinear least-squares algorithm (KaleidaGraph™) for the fitting process. Figure 2 shows the resulting fitted functions and the FWHM data. Table 3 records the parameters for the generalized Padé approximant forms fitted to the SNS FWHM functions.

[‡] Much is known about Padé approximants. Consult Wikipedia and references cited there under this topic.

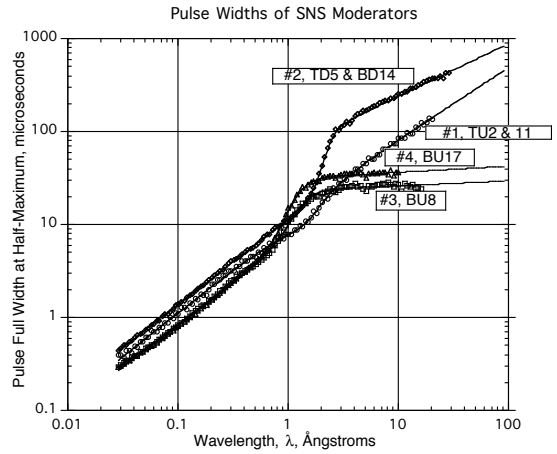

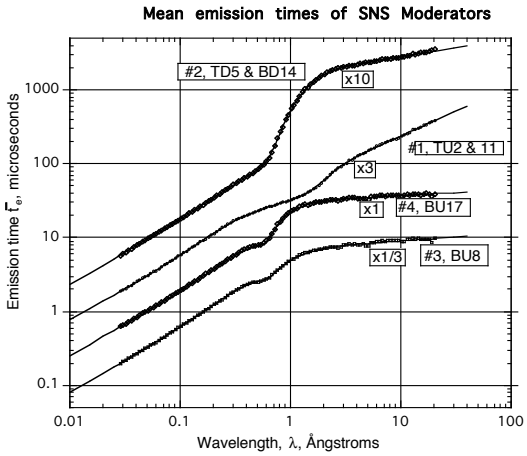

Figure 2 (left). Pulse full FWHMs for the four distinctly different SNS viewed moderator surfaces. Figure 2 (right). Mean emission time t_e vs. wavelength for SNS moderators, and the fitted functions. (Data courtesy E.B. Iverson.)

Table 3. Parameters of the fitted FWHM functions for SNS moderators

Parameter	#1 TU 2 & 11	#2 TD 5 & BD 14	#3 BU 8	#4 BU 17
a	10.14	11.46	6.60	6.58
b	0.949	0.919	0.892	0.898
c, $Å^{-1}$	-0.744	0	0	0
d, $Å^{-2}$	0	0	0	0
e, Å	1.878	1.892	1.042	8.60
q	2.98	7.91	3.97	4.45
c′, $Å^{-1}$	-0.578	0	0	0
d′, $Å^{-2}$	0	0	0	0
e′, Å	1.995	2.279	1.343	1.182
q′	3.152	8.26	4.81	5.28

The fitted functions are quite accurate renderings of the calculated data, although, because there are a large number of parameters, there are sizable correlated errors in the fitted parameters.

Mean emission times

Neutrons emerge from the moderator surface after (recall causality) the exciting fast-neutron pulse in a time distribution that depends on the wavelength. The mean time of arrival of neutrons in the detectors of a scattering instrument depends on the wavelength and flight path length to first order, but delayed by the mean time of emission from the nominal moderator surface (depends on the definition of that surface). In turn, the wavelength calibration of the instrument depends on the mean emission time and in some instruments (e.g., high-resolution time-of-flight powder diffraction) requires considerable precision. Figure 2 (right) shows the mean emission times for the four distinctly different SNS viewed moderator surfaces.

Table 4 summarizes the values of the parameters of the functions fitted to the calculated mean emission times of the four distinctly different viewed SNS moderator surfaces.

Table 4. Parameters of the fitted emission time delay functions for SNS moderators

Parameter	#1 TU 2 & 11	#2 TD 5 & BD 14	#3 BU 8	#4 BU 17
a	10.02	12.268	10.99	11.486
b	0.798	0.864	0.830	0.830
c, $Å^{-1}$	0.7623	-1.6811	-0.6462	-0.9154
d, $Å^{-2}$	4.401	0.4643	-2.585	-1.5565
e, Å	1.2781	0.8349	0.6542	0.7191
q	6.890	5.662	4.459	5.429
c′, $Å^{-1}$	-1.3972	-2.316	-2.202	-2.2231
d′, $Å^{-2}$	6.196	1.7031	1.1174	1.2939
e′, Å	1.3703	1.2836	0.7924	0.8772
q′	7.023	6.290	5.193	6.176

As in the earlier cases, the fitted functions are quite accurate renderings of the calculated data, but because there are a large number of parameters, there are sizable correlated errors in the fitted parameters.

In practice, accurate accounting for spectral intensities, pulse FWHMs, and especially mean time delays, may require fits to measurements as opposed to the simulations treated here. This is likely—reality differs from the calculated results and fitted functions. Then the fitted forms, considering the results here as successful tests, may serve good purposes. Parameters in the modified Westcott function describing spectral intensities and the generalized Padé approximants describing resolution broadening widths and mean emission times might be refined simultaneously with sample physics model parameters in day-to-day experimental procedures. It is well to remember that measured beam intensity measurements must allow for attenuation by air and solid materials in the beam that are not accounted for in the simulations. Similarly, wavelength calibration measurements need to allow for electronic time delays and delays due to finite detector thickness (see *Elements,* Chapter 8, Detectors).